applied sciences

Article

Diagenesis of Deep Low Permeability Reservoir in Huizhou Sag and Its Influence on Reservoirs

Shan Jiang [1,2], Rong Guo [1,2], Shuyu Jiang [1,2] and Jun Cai [1,2,*]

[1] Cooperative Innovation Center of Unconventional Oil and Gas, Yangtze University, Ministry of Education and Hubei Province, Wuhan 430100, China; shanjiang1012@163.com (S.J.); guorong0214@163.com (R.G.); shuyujiang0916@163.com (S.J.)
[2] School of Geosciences, Yangtze University, Wuhan 430100, China
* Correspondence: 2022710412@yangtzeu.edu.cn

Abstract: The Paleogene Enping Formation in the Huizhou Sag, Pearl River Mouth Basin, has been identified as a key target for deep oil and gas exploration. However, research on the diagenesis of these deep reservoirs still remains limited. This study evaluated the role played by diagenetic processes on the reservoir quality of the Paleogene Enping Formation in the Huizhou Sag, Pearl River Mouth Basin, from braided river deltas to meandering river deltas. A core observation, thin section examination, cathode luminescence analysis, scanning electron microscopy, mercury penetration, porosity–permeability test, and other analytical methods were performed to analyze the diagenesis and its impact on the physical properties of the deep, low-permeability sandstone reservoirs in the Enping Formation within the study area. It was shown that the reservoir composition maturity of the Paleogene Enping Formation in Huizhou Sag is relatively high, and the reservoir space is dominated by dissolved pores, accounting for more than 48.2%. The deep and ultra-deep clastic reservoirs are typically characterized by "low porosity, low permeability, and strong heterogeneity". In particular, the reservoir space of the deep, low-permeability reservoir of the Enping Formation is significantly affected by diagenesis in which mechanical compaction notably altered the porosity of the Enping Formation reservoir, with a reduction in pore volume ranging from 12.5 to 27.2% (average 18.9%); cementation usually enhances pore reduction by between 2.1 and 28.7% (average 11.7%), while dissolution has resulted in an increase in pore volume ranging from 1.4 to 25.6% (average 10.1%). A further analysis revealed that the deep reservoir type in this region is characterized by "densification", as evidenced by the correlation between reservoir porosity–permeability evolution and hydrocarbon accumulation.

Keywords: Huizhou Sag; deep reservoir; diagenesis; Pearl River Mouth Basin; tight sandstone

Citation: Jiang, S.; Guo, R.; Jiang, S.; Cai, J. Diagenesis of Deep Low Permeability Reservoir in Huizhou Sag and Its Influence on Reservoirs. *Appl. Sci.* **2024**, *14*, 11656. https://doi.org/10.3390/app142411656

Academic Editor: Andrea L. Rizzo

Received: 9 November 2024
Revised: 12 December 2024
Accepted: 12 December 2024
Published: 13 December 2024

1. Introduction

The diagenesis of clastic rock reservoirs and its impact on reservoirs' physical properties has always been a research hotspot and a challenging topic, which is of great significance for deep oil and gas exploration and development [1–4]. The continuous advancement in oil and gas exploration technology has led to the discovery of an increasing number of deep and ultra-deep oil and gas resources. These newly discovered areas are poised to become significant contributors to the global reserves and production of oil and gas [5–9]. Compared with conventional reservoirs, deep clastic rock reservoirs have undergone a more complex diagenetic process and are often characterized by "low porosity, low permeability, strong heterogeneity" [10,11]. Although destructive diagenesis can cause the physical properties of deep reservoirs to deteriorate, they can still become high-quality reservoirs under specific conditions [12–16]. Therefore, studying the diagenesis of deep clastic rock reservoirs and its impact on reservoirs' physical properties can help effectively predict the distribution of favorable reservoir zones so as to provide a reliable geological basis for deep oil and gas exploration.

Currently, it is generally suggested that factors such as particle size, sorting degree, and compositional components affect the initial properties of tight sandstones [17,18]. Diagenesis, however, plays a pivotal role in determining their final characteristics, exerting significant control over the heterogeneity and reservoir properties of deep clastic rock reservoirs [18,19]. The relationship between diagenesis and reservoir quality is mainly reflected in the impact of different types of diagenetic processes on pore development and pore evolution in the reservoirs [20,21]. Generally speaking, deep sandstone reservoirs are controlled by compaction and cementation, leading to reduced porosity and permeability, and resulting in the reservoirs having poor physical properties overall [22–25]. However, many scholars have found that there are a large number of primary pores and secondary dissolution pores in deep sandstone reservoirs, effectively improving the performance of the reservoirs [26,27]. For instance, grain coatings composed of authigenic clay minerals (chlorite and microcrystalline quartz) often prevent contact between the grain surface and diagenetic fluids, inhibiting the occurrence of cementation, thereby playing a crucial role in preserving primary pores [28–30]. Yan Zhenghe et al. conducted experiments on the mechanical properties of offshore loose sandstone reservoirs [31]. Their research suggests that the abnormally high pressure that developed in the deep layers effectively slowed down the occurrence of cementation, resulting in distinct zones of high-quality reservoir development [31]. Ortiz-Orduz et al. studied the Cachiri Group's tight sandstone reservoirs and found that the dissolution of carbonates and feldspars produced secondary pores, enhancing the reservoir quality in the region [32]. Although a large number of primary and secondary pores are found in deep sandstones, their diagenesis is still subjected to comprehensive control by various factors such as basin properties, tectonic evolution, sedimentary types, burial processes, fluid properties, and diagenetic physical and chemical environments in different regions [33–36]. Therefore, more detailed research should be conducted on the types of diagenesis in different regions and their impact on reservoir performance so as to effectively guide the exploration and development of deep oil and gas resources.

The Huizhou Sag, located in the Pearl River Mouth Basin, has demonstrated significant potential for oil and gas exploration and development (Figure 1C), having achieved notable results since the initiation of its production. The deep, low-permeability sandstone reservoirs of the Paleogene Wenchang Formation and Enping Formation contain vast amounts of oil and gas resources, accounting for over 30% of the total natural gas resources in the depression [37]. Currently, the focus of oil and gas exploration and development in the entire Pearl River Mouth Basin's Huizhou Sag is on the deep and ultra-deep layers of the Enping Formation [37]. Previous studies have been conducted on the provenance conditions, sedimentary characteristics, hydrocarbon accumulation, and reservoir prediction of the Enping Formation [37,38]. It is posited that the sand bodies formed under the braided river sedimentary environment of the Enping Formation are the material basis for the formation of deep, low-permeability reservoirs. The reservoirs exhibit characteristics of being initially tight followed by accumulation, and oil is ubiquitous throughout the region [37–39]. Although there are many studies on the controlling factors of the deep reservoirs in the Enping Formation, research on these controlling factors is relatively superficial, and the impact of diagenesis on pore development is not clear [38]. Therefore, based on a comprehensive core analysis of test data from nine wells combined with previous research, this paper systematically studies the diagenesis of the deep, low-permeability sandstone reservoirs of the Paleogene Enping Formation in the Huizhou Sag and its impact on the reservoir. This study aims to elucidate the controlling factors of reservoirs' physical properties in the study area, thereby providing valuable geological support for deep oil and gas exploration in this block.

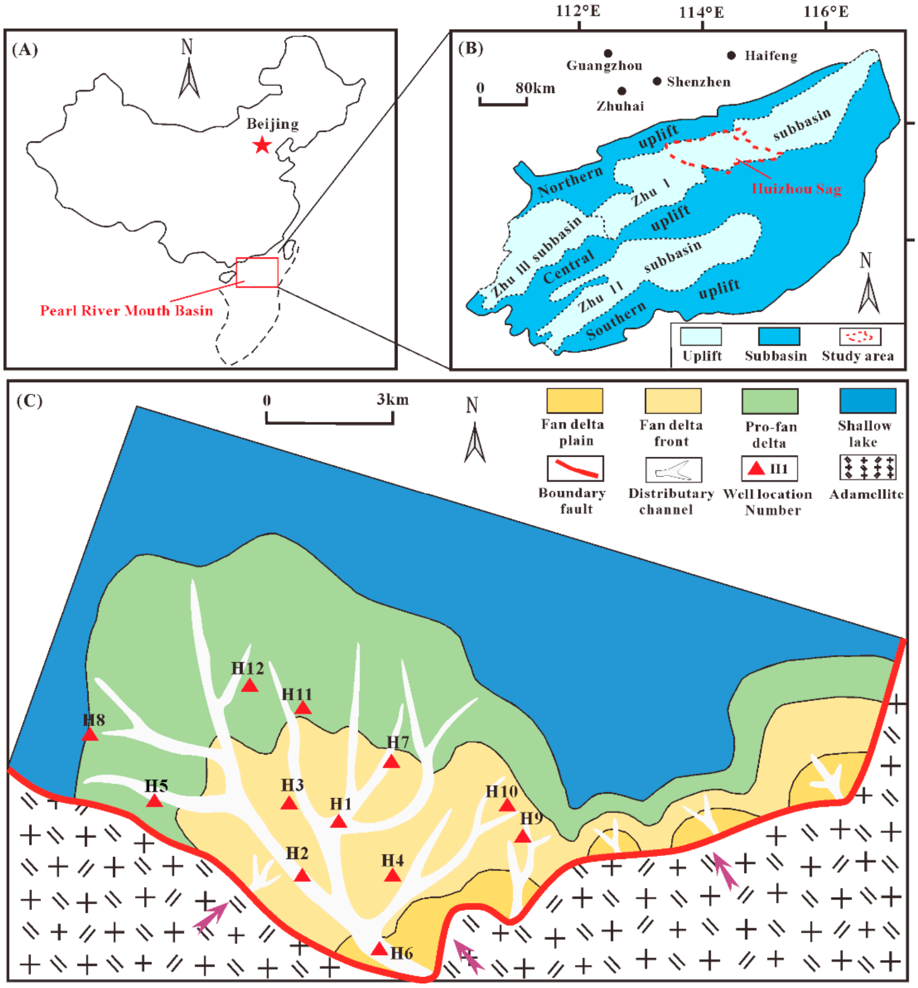

Figure 1. A structural map of the Huizhou Sag in the Peral River Mouth Basin [37]. (**A**) The geographical location of the Pearl River Mouth Basin. (**B**) A location map of the Huizhou Sag, the Pearl River Mouth Basin. (**C**) The locations of the study area and sample well.

2. Geological Background

2.1. Tectonics

The Pearl River Mouth Basin is located on the southern margin of the Chinese continent (Figure 1A). Its basement is the Yanshanian rock mass and Paleogene fold. The tectonic zone is bounded by the XiJiang Sag to the west, the Huilu Low Sag to the east, the Dongsha Sag to the south, and the North Fault Terrace to the north. The tectonic zone is a large-scale meso-Cenozoic sedimentary basin with a length of about 800 km, a width in the range of 100–300 km, and a total area of approximately 7400 km^2 [40]. It consists of four depression zones, including the Zhu-I Depression, the Zhu-II Depression, the Zhu-III Depression, and the Chaoshan Depression, and three uplift zones, including the North Uplift Zone, the Central Uplift Zone, and the Southern Uplift Zone (Figure 1B). The Huizhou Sag is located in the southwest part of the Zhu I Sag, a set of simple fault depression basins formed since the early Tertiary [41]. The geological evolution of the Huizhou Sag has been significantly influenced by the Philippine Sea Plate, Eurasian Plate, and Indo-Australian Plate. In the Cenozoic era, it mainly experienced three tectonic events: the continental rift stage, the Paleogene and Miocene passive continental margin stage (post-rift stage), and the Late Miocene–Quaternary Neotectonic stage. It encompasses five depressions (Huixi, Huibei, Huinan, Huidong, and Luxi) and two uplifts (Huizhong and Huidong) [40,41].

2.2. Stratigraphy and Sedimentology

Due to the influence of strong tectonic activities, the Huizhou Sag developed the Paleocene Shenhu Formation (SH), the Eocene Wenchang (WC) and Enping Formations (EP), and Oligocene Zhuhai Formation (ZH) during the continental rift stage. Among them, the Eocene Wenchang and Enping Formations are the most important source rocks, which consist of lacustrine mudstone, fluvial sandstone, and coal in an interbedded manner [40]. The Oligocene Zhuhai Formation consists of deltaic coastal siltstone and is the main reservoir in the Huizhou Sag. During the passive continental margin stage, the Miocene marine siltstone, mudstone, and carbonate Zhujiang (ZJ) and Hanjiang (HJ) Formations were developed in the Huizhou Sag. The Miocene Yuehai (YH) Formation, Pliocene Wanshan Formation (WS), and Quaternary sediments were deposited in a marine environment during the neotectonic stage (Figure 2). From the Paleocene to the Neogene, there were three sets of oil source rock, reservoir, and caprock. Influenced by regional extensional forces, the Huizhou Sag was a lake basin during the Eocene Wenchang Formation deposition period, and high-quality lacustrine hydrocarbon source rocks were widely developed during this period. Subsequently, the paleolake basin gradually shrank during the Eocene Enping deposition period, and fluvial deltas were developed in most areas (Figure 1C) [39,40].

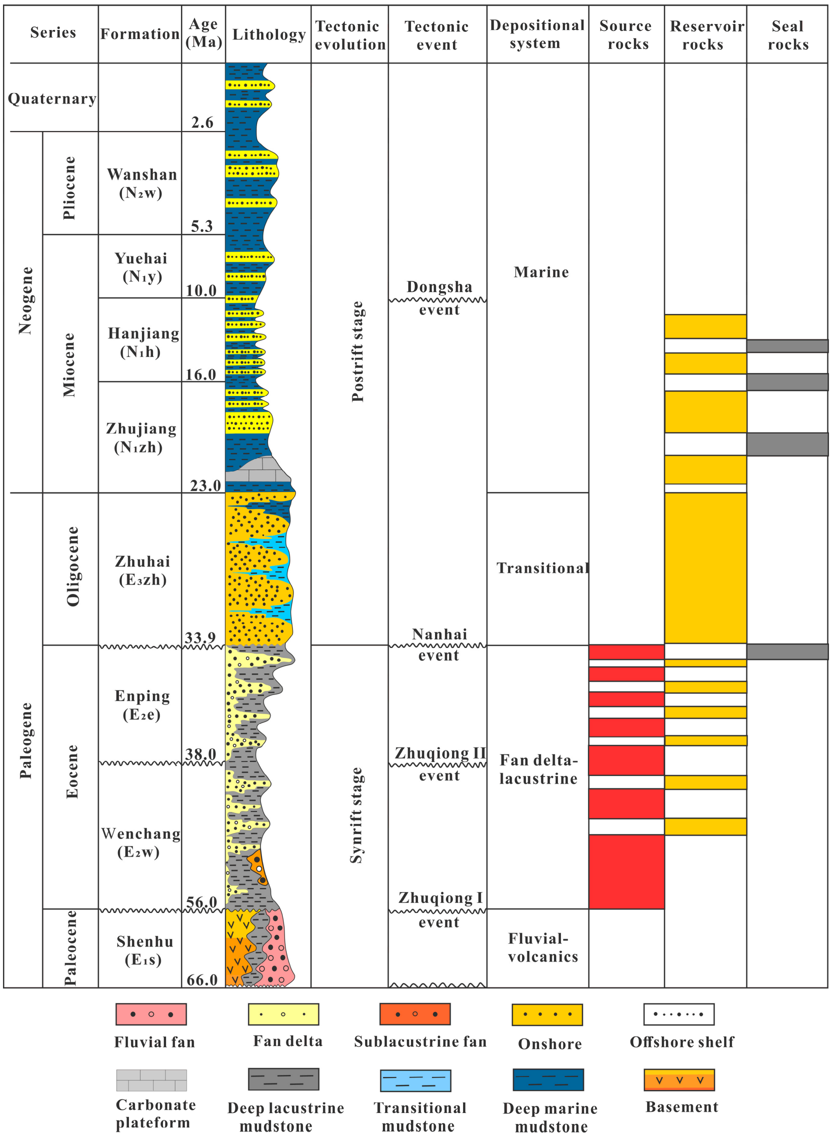

Figure 2. Comprehensive column chart of strata in Huizhou Sag, Pearl River Estuary Basin [41,42].

The formation studied in this paper is the Enping Formation, which has a maximum thickness in the range of 2062.7–4184.8 m, with an average burial depth of 3259.2 m [38,39]. An analysis of the Enping Formation revealed that the Enping Formation is a product of the transitional stage. The sedimentary facies were dominated by subaqueous distributary channels and mouth bars and consisted of a depositional environment characterized as deltaic and lacustrine deposits. The Enping Formation is a sandstone-dominated stratum of generally thick sand conglomerate and fine-medium sandstone, with occasional layers of siltstone and mud [38,43,44]. The target interval lies within an underwater low rise, which is characterized by a shallow water depth, a relatively flat terrain, and strong lake wave movement conducive to beach bar development (Figure 1C). Therefore, a sensitivity investigation of the deep layers is vital for deep oil and gas exploration in this area.

3. Database and Methods

In this study, we conducted a comprehensive analysis of the Enping Formation using drilling and logging data from nine coring wells (H1–H9) in conjunction with laboratory data derived from 114 core samples obtained from the Huizhou Sag (Figure 1C). The experimental methods employed included thin-section petrography, scanning electron microscopy (SEM) imaging, X-ray diffraction (XRD) analyses, and porosity–permeability tests. All data pertaining to thin-section samples, as well as reservoir porosity and permeability, were sourced from the Shanghai Branch of CNOOC Ltd., Shanghai, China.

Following the vacuum impregnation of each core sample with blue epoxy resin, thin sections were meticulously prepared for the comprehensive analysis of petrological characteristics, grain structure, pore morphology, diagenesis, and visual porosity. Selected sections underwent staining with Alizarin Red to facilitate the identification of carbonate minerals. The presence and nature of authigenic clay minerals, micropores, and microfractures were scrutinized utilizing a scanning electron microscope (SEM). A cathode luminescence (CL) analysis was conducted on 65 samples to assist in elucidating the paragenetic sequence. An automated permeameter–porosimeter, AP-608, was employed to investigate the porosity and permeability of samples derived from various structural zones and members.

Point counts were performed on thin sections to quantify the content of detrital grains and carbonate cement, with at least 300 points counted. The scanning electron microscopy (SEM) experiment was conducted using an FEI Helios NanoLab 660 Dual Beam SEM equipped with an energy-dispersive X-ray spectrometer to identify the main types of authigenic minerals and different pore spaces. The samples were observed under SEM at an acceleration voltage of 20 keV to characterize the pore geometry and cement morphology and document the textural relationships between minerals. Core samples were dried and freshly broken, and their surfaces perpendicular to the bedding plane were coated with chromium before SEM and TIMA observations. Cathodoluminescence (CL) analysis was performed using a Technosyn cold cathode luminoscope to identify different generations of cement. This test was performed according to the Chinese trade standard for tight sandstone gas engineering (SY/T6832-2011) [45].

Porosity and Permeability Assessment: The assessment of porosity and permeability was conducted utilizing an automatic porosimeter (AP-608) (Beijing Ordovician Technology Co., Ltd., Beijing, China) and a permeability analyzer (K02GS006) (Best Instrument Technology Co., Ltd., Beijing, China). The detection limits for these instruments were not less than 0.1% and ranged between 0.05 and 10,000 mD, respectively.

4. Results

4.1. Basic Characteristics of Reservoir

4.1.1. Reservoir Lithology and Physical Characteristics

The observation of nine thin sections (H1–H9) in the Huizhou Sag and a statistical analysis conducted on the microscopic characteristics of the rock slices show that reservoir rocks in the Enping Formation have more than a 70% content of quartz in the sandstone of the Enping Formation, while there are smaller contents of feldspar and rock debris.

Compositionally, the sandstones dominantly include feldspar quartz sandstone, lithic quartz sandstone, lithic feldspar sandstone, and feldspar lithic sandstone, as determined using an analysis of the X-ray diffraction data of 31 rock samples from the Enping Formation in the Huizhou Sag (Figure 3).

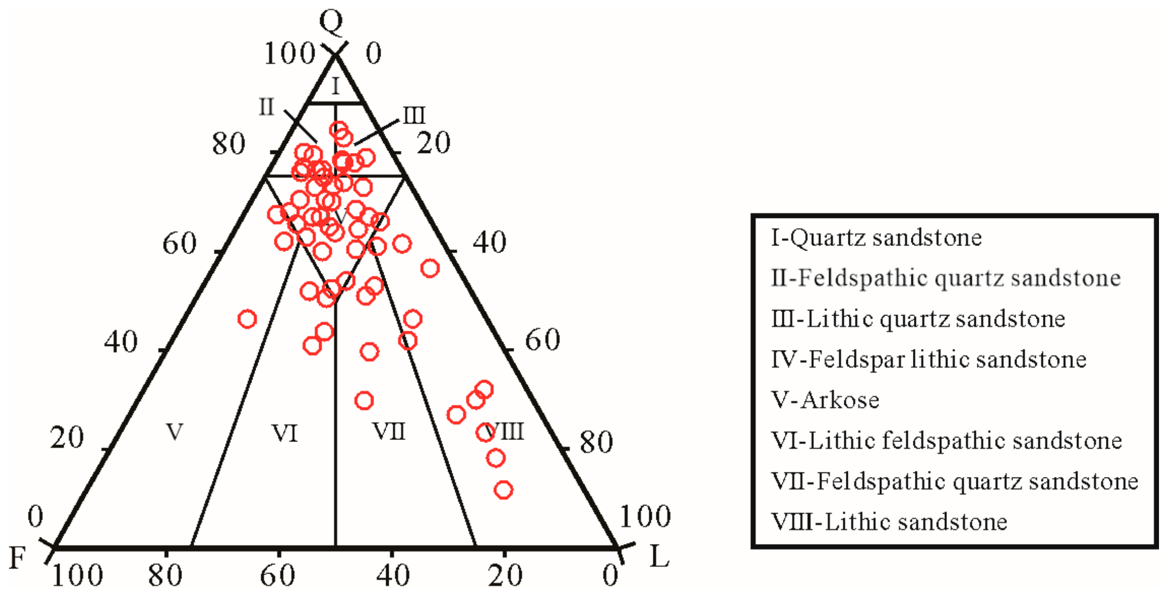

Figure 3. Rock component projection map and sandstone types of Enping Formation in Huizhou Sag. Q—Quartz; F—Feldspar; L—Lithic.

The measurement results of rock porosity show a distribution range of 1.1–19.8%, and the permeability is about 0.0017~612.02 $\times$ 10^{-3} μm^2. Through careful observation, it is evident that the porosity and permeability increase with depth in response to various compaction processes. At shallow burial depths, the compaction trend shows good agreement with the experimental compaction of loose Enping sand, indicating that effective stress is the controlling factor of the physical properties at shallow depths. However, in areas where the stratum depth exceeds 3500 m, porosity and permeability still have a good correlation. This suggests that there are areas with relatively high quality throughout the low-porosity and low-permeability reservoirs that have great exploration potential. In conclusion, the reservoir is generally a porous reservoir with low porosity and permeability (Figure 4).

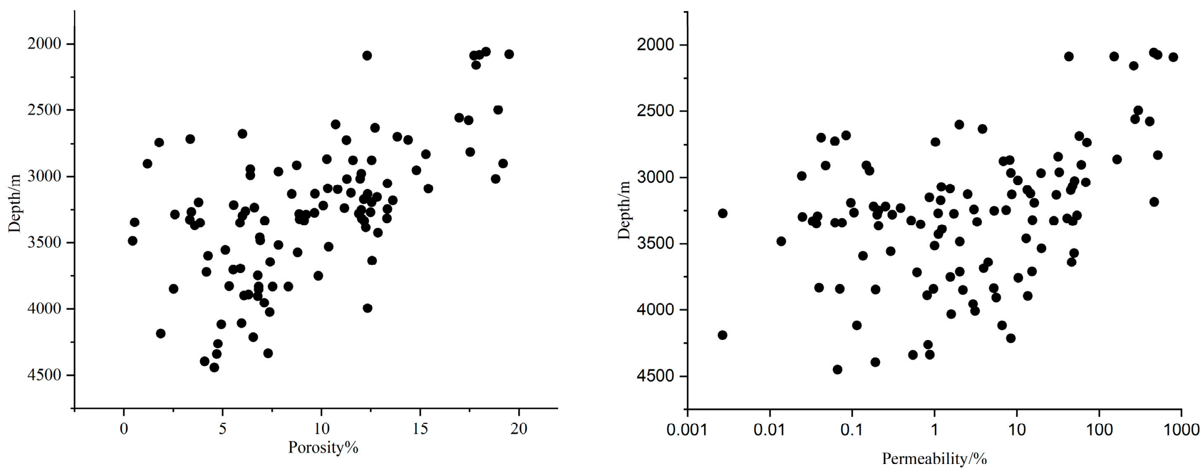

Figure 4. Physical characteristics of sandstone of Enping Formation in Huizhou Sag.

4.1.2. Reservoir Space Characteristics

According to a comprehensive analysis of 105 rock samples from the Enping Formation, for example, the deep low permeability reservoir of the Enping Formation is characterized by a porous reservoir. In the samples, the pores mainly included primary intergranular pores (19.8%), intergranular dissolved pores (27.1%), dissolved pores in grains (10.9%), kaolinite intergranular pores (12.3%), mold pores (18.1%), matrix micropores (3.2%), microcracks (3.1%), and fewer diagenetic fractures (4.2%). However, the Enping Formation contained a high proportion of primary intergranular pores, with an average of 25.25%, which play a vital role in the formation and development of reservoirs. The microscopic observations revealed that primary intergranular pores are mainly developed in quartz-rich sandstones such as feldspar quartz sandstone ($Q_{76}F_{16}L_8$) and lithic quartz sandstone ($Q_{67}F_{15}L_{18}$), and there is no calcareous or clay cementation between the skeleton particles. Ultimately, dissolution pores are the essential type of reservoir space, which have a significant influence on the reservoir's physical properties, and their porosity contribution rate is approximately 48% (Figure 5).

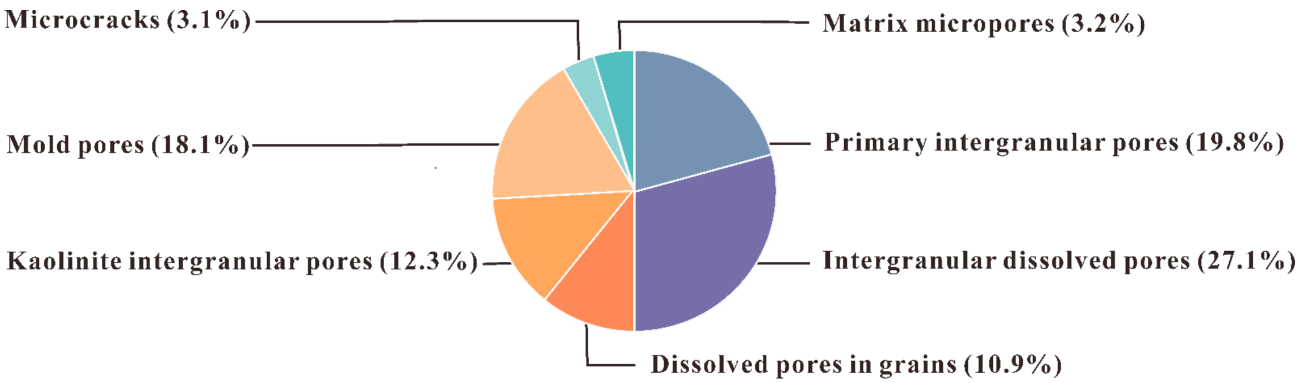

Figure 5. Pore types in Enping Formation in Huizhou Sag.

4.2. Diagenetic Processes

Diagenesis, which exerts strong control on the evolution of pore structure and the alteration in the physical and chemical properties of clastic rock, is controlled by a variety of chemical, physical, and biochemical interactions [46–49]. Currently, an important driving force for researching deep reservoir diagenetic studies in the Paleogene Enping and Wenchang Formations is the efficient exploration and exploitation of the deep and ultra-deep reservoirs (exceeding 3500 m) in the Pearl River Mouth Basin [39]. The low-permeability sandstone reservoirs in Huizhou Sag of the Pearl River Mouth Basin have undergone various diagenesis processes [38]. However, the main diagenesis types are still compaction, cementation, and dissolution, which significantly influence the reservoir quality (Figure 6).

4.2.1. Compaction

Compaction includes mechanical compaction and chemical compaction, acting throughout the entire diagenetic process. It is a significant diagenetic process in clastic rock reservoirs, influencing the entirety of pore formation, evolution, and preservation in sandstone reservoirs. Among them, mechanical compaction is explained by the fact that sandstones become compacted under the weight of the overlying strata by grain displacement and deformation so that porosity is reduced relatively and even leads to their densification [50,51]. The intensity of mechanical compaction is related to the rock composition, reservoir depth, geothermal gradient, and tectonic stress in the study area. The inequigranular sandstone has a high mud matrix content and is less sortable, while the compaction effect is high, so the mud matrix and finer grains are squeezed into the space among coarser grains, reducing the porosity (Figure 6A,B). Line contact among grains is dominant, and some grains are fracted (Figure 6C).

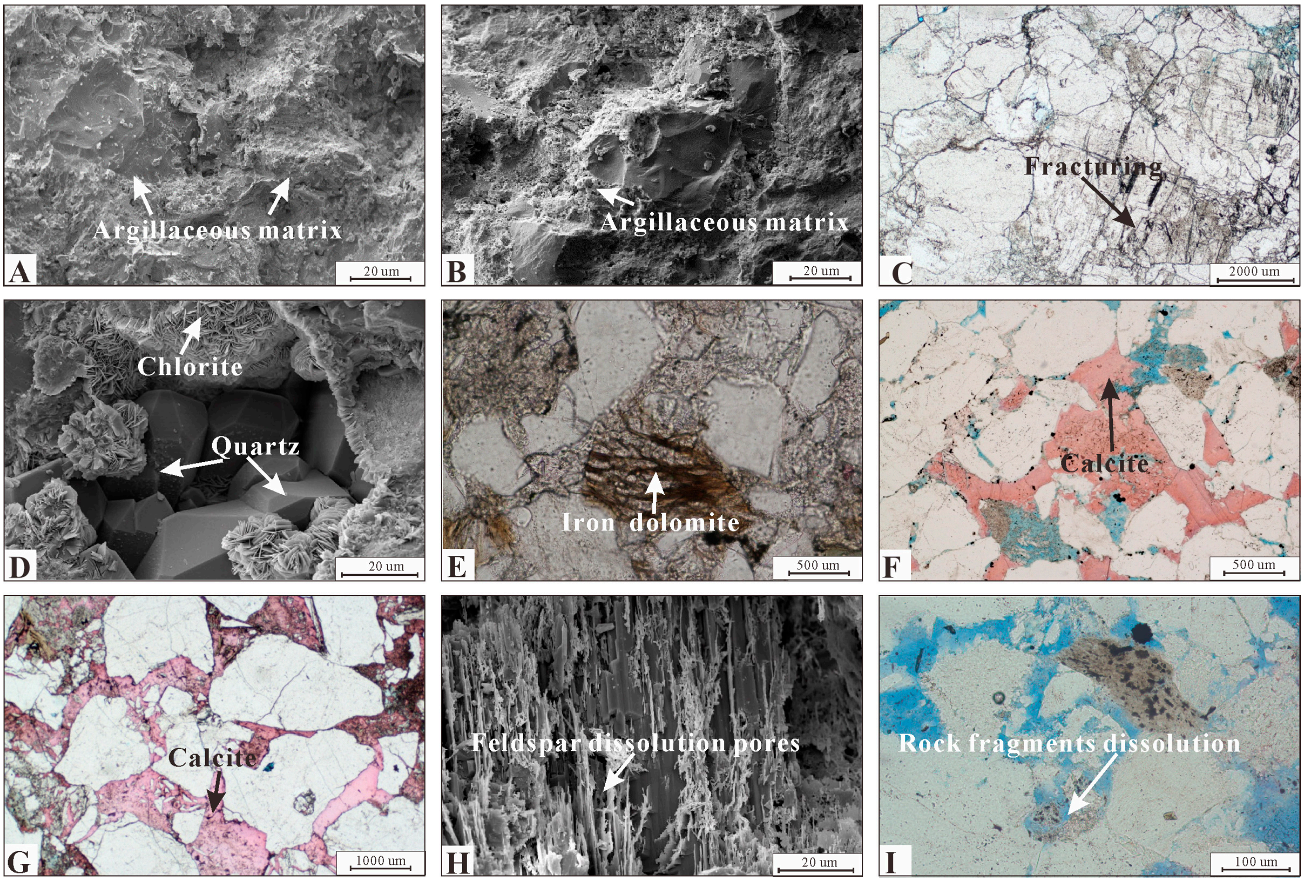

Figure 6. Photomicrographs and SEM images of the Enping Formation in Huizhou Sag sandstone: (**A**) Well Y8, 3392 m, with a high argillaceous matrix content and a dense structure; (**B**) Well Y5, 3546.3 m, with a high argillaceous matrix content contact between clastic particles; (**C**) Well Y1, 3601 m, where intense compaction causes the rock to form fractures; (**D**) Well Y4, 3541.3 m, which has microcrystalline quartz and lamellar chlorite aggregate; (**E**) Well Y8, 3313 m, which has intergranular pores filled with cement ferridolomite grains; (**F**) Well Y6, 3507 m, where the clastic particles are in point contact, and carbonate cement is developed; (**G**) Well Y9, 3374.7 m, where the formed intergranular pores are filled with carbonate cement; (**H**) Well Y4, 3684.5 m, with a feldspar solution hole; and (**I**) Well Y5, 3550.1 m, with pores formed by rock debris dissolution.

4.2.2. Cementation

The cementation of low-permeability sandstone reservoirs in the Huizhou Sag is commonly observed, with cementation occurring in various structural well areas and at different burial depths. Siliceous cementation, carbonate cementation, and a small amount of clay mineral cementation (such as some chlorite grain coating clay minerals filled amidst clastic particles) (Figure 6D) are the main types of cement. Specifically, siliceous cementation zones are mainly concentrated in the diagenetic stage between burial depths in the range of 1550–3200 m, while carbonate cementation primarily occurs in the medium diagenetic stage between burial depths in the range of 2920–4280 m.

Silica Cementation

The siliceous cementation of the Enping Formation is mainly characterized by quartz secondary overgrowths, while authigenic quartz minerals in primary intergranular or dissolution pores are rare. Under scanning electron microscopy, it can be observed that the quartz secondary enlargement is arranged in an embedded manner (Figure 6D). It is evident that quartz crystals grow towards the pore spaces, and the width of the enlarged edge of quartz (mainly grade II) ranges from 4 to 38 μm. Furthermore, it was noted that the thickness increased with the burial depth, indicating its influence on multi-stage acidic fluids during burial. Previous studies have shown that siliceous material in clastic rock reservoirs is mainly derived from the pressure dissolution of quartz particles and feldspar mineral dissolution in an acidic environment [52,53]. Specifically, unstable potassium feldspar and albite dissolved in an acidic environment to form SiO_2 [52]. The formation formula is as follows.

$$2KAlSi_3O_8 + 2H^+ + H_2O \rightarrow AL_2Si_3O_5(OH)_4 + 4SiO_2 + H_2O + 2K^+ \quad (1)$$

$$2NaAlSi_3O_8 + 2H^+ + H_2O \rightarrow AL_2Si_3O_5(OH)_4 + 4SiO_2 + H_2O + 2Na^+ \quad (2)$$

Carbonate Cementation

The evidence from the thin section and SEM indicates the presence of different types of carbonate cement in the dense, low-permeability sandstone reservoirs of the Enping Formation in the Huizhou Sag. For example, the early formation of some brown iron dolomite cement and red carbonate cement between clastic particles can be seen (Figure 6E–G). A microscopic examination revealed that the total proportion of calcite cementation is pervasively developed in the Enping Formation as an important feature of carbonate cementation, showing different formation levels depending on the depth at which they are buried. The microscopic results indicate a lack of primary pore development, with detrital particles mainly in point contact and relatively weak mechanical compaction (compaction amount < 27.8%), which suggests that calcite cement inhibits mechanical compaction when the content of calcite cement exceeds 9.8% in the study area. In the early stage of diagenesis, calcite cement occupied in sandstone is generally formed from dissolved calcium components in pore water in open environmental conditions during the early diagenetic stage (burial depth < 1000 m) [53,54], whereas in the later stages, calcite cement is mainly occupied by cementation resulting from the pressure dissolution of carbonate particles [53]. The occurrence of calcite cement in the Enping Formation reservoir in Huizhou Sag is attributed to early pore water.

4.2.3. Dissolution

The dissolution of all soluble components in sandstone occurs under specific environmental conditions in secondary pores, which can improve the reservoir performance of sandstone. In particular, dissolution is of great significance in low intergranular pore sandstone reservoirs in forming secondary pores and developing “sweet spots” [55,56]. In the study area, the tight sandstone reservoirs in the Enping Formation section obviously undergo diagenetic modification through dissolution. Specifically, from the scanning electron microscope analysis, secondary dissolution pores, predominantly pores in the grain, are feldspar dissolved along the cleavage plane, and the unstable components in the cuttings are dissolved, forming pores with honeycomb and patch distribution (Figure 6H,I). In the Enping Formation, the contribution of potassium feldspar mineral particle dissolution to secondary dissolution pores is primary, and that of debris is secondary, whereas the proportion of dissolution fractures is rare (Figure 5).

4.3. Diagenetic Stage and Diagenetic Sequence

According to the diagenetic stage classification criterion and the Chinese standard classification scheme of sandstone diagenesis, “the division of diagenetic stages of the clastic rocks” (SY/T5477-2003) [57] based on the current industry standards, combined with the distribution characteristics of cement, the contact relationship of clastic particles (point contact, line contact, and concave–convex contact), the diagenetic sequence of the Enping Formation in Huizhou Sag has been reconstructed (Figure 7). In conclusion, the reservoirs in the study area are in the stage of middle diagenesis A–B.

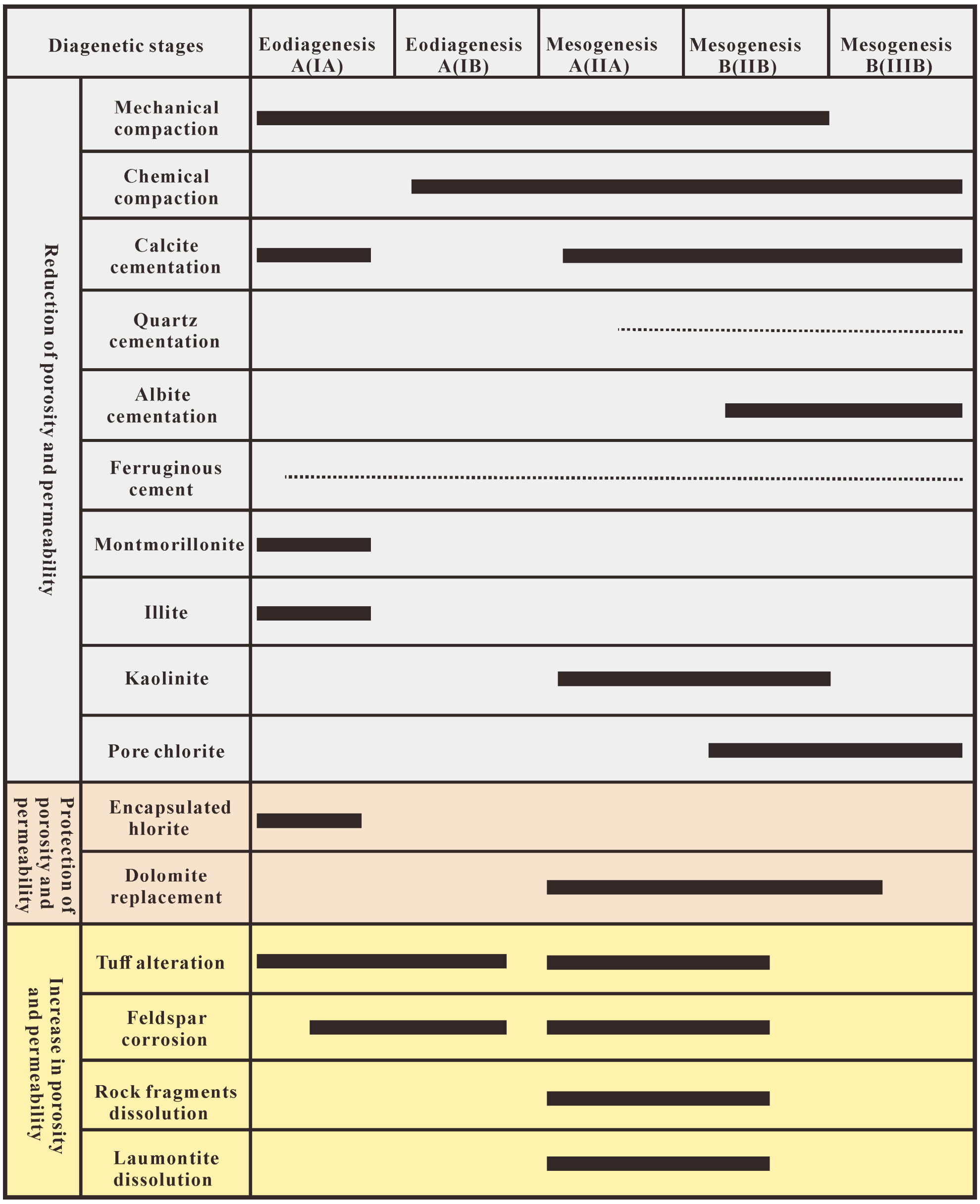

Figure 7. Diagenetic sequence of sandstone reservoir of Enping Formation in study area.

In early diagenesis stage A (IA), the reservoir had a shallow burial depth, where a weak alkaline environment gradually transformed montmorillonite into illite, and mechanical compaction significantly transformed the pore space. The formation water, which contains a substantial amount of alkali metal ions (Na^+ and K^+), will undergo acidic dissolution with pyroclastic materials, resulting in a small amount of chlorite film and secondary quartz enlargement, while the pore water in the sediments will precipitate and form micritic calcite.

In early diagenesis stage B (IB), a large amount of montmorillonite was transformed to create an illite–montmorillonite mixed layer. In addition to authigenic clay minerals, small amounts of siderite and quartz minerals were also formed. At the same time, the whole sandstone was unconsolidated—and it was mostly weakly consolidated in loose sand—and the clastic particles were mainly in point contact. In middle diagenesis stage A (IIA), with the burial depth, the development degree of the source rocks gradually matures, and the amount of organic acids gradually increases. Pore water discharges a significant amount of organic acids, leading to the corrosion of soluble minerals like potassium feldspar and plagioclase. The relatively enclosed diagenetic environment delays the discharge of the precipitated material resulting from dissolution, leading to the formation of various types of cement, including kaolinite, illite, quartz, and calcite.

In middle diagenesis stage B (IIB) of the Enping rock formation, the relatively closed diagenetic environment gradually changed, showing a weak alkaline environment and leaf-like chlorite precipitating in intergranular and dissolution pores. Meanwhile, dolomite metasomatism, calcite, and quartz occurred.

The diagenetic evolution sequence of the Enping Formation reservoir is as follows: it starts with early diagenetic stage A (IA), which involves mechanical compaction and the formation of a chlorite film; then, it moves on to early diagenetic stage B (IB), where mechanical compaction, tuffaceous alteration, and the dissolution of feldspar occur; then, it moves on to middle diagenetic stage A (IIA), which involves chemical compaction, dolomite cement, feldspar dissolution, debris dissolution, and kaolinite consolidation; and then it moves on to late diagenetic stage B (IIB).

5. Discussion

5.1. Impact of Compaction on Reservoir Quality

Previous studies have established a quantitative relationship between the primary pore volume of sandstone (V_1) and the sorting coefficient (S_0) to determine the primary pore volume (initial intergranular volume or initial depositional porosity) of clastic sediments [58]. The grain size statistics based on the clastic particle size classification show that the distribution of the sorting coefficient of Enping Formation sandstone ranges from 1.45 to 14.8 with an average value of 2.35. Therefore, we can deduce that the initial porosity of deep, low-permeability Enping Formation sandstone spans from 24.6 to 36.1% with an average value of 26.8%. Because of the reservoir effect caused by mechanical compaction, the sandstone particles were packed together, and the initial porosity decreased or even disappeared. However, the pores that were not affected by mechanical compaction stayed the same. Mechanical compaction in the Enping Formation affected the residual porosity (V_2), which primarily consists of the remaining primary intergranular pores and early cementation-preserved pores.

$$V_2 = \frac{P_1 + P_c}{P_t} \times Q_m + W \tag{3}$$

$$V_{mc} = V_1 - V_2 \tag{4}$$

The formula shown above uses a thin slice of the cast material under a microscope to calculate the percentage of the remaining intergranular pore surface, represented as P_1 and expressed in %. By examining a thin slice of the cast material under a microscope, we can determine the ratio of the pore face area occupied by carbonate cement dissolution, which we express as P_C in %. We represent the content of cement that controls the reservoir property analyzed by a thin slice of the cast material under a microscope, expressed as W in %. P_t represents the total face percentage obtained from analyzing a thin slice of the cast material under a microscope, expressed in %; Q_m represents the measured porosity within the core samples, expressed in a percentage; V_1 represents the original porosity level before mechanical compaction occurred, expressed in %; and V_2 represents the porosity level after mechanical compaction and is expressed in %, while V_{mc} represents the amount of porosity lost due to mechanical compaction processes, also expressed in %. Microscopic observations reveal a loss range of 12.5–28.2% due to compaction processes, with an average value of 18.9.

5.2. Impact of Cementation on Reservoir Quality

The analysis of cementation revealed that the calcareous and siliceous cement formed in the IIA–IIB stages of diagenesis primarily fills the intergranular dissolved pores, intragranular dissolved pores, and melodic pores formed in the IB–IIA stages of diagenesis. Cementation results in a reduction in the pore space, where the volume of cement is equivalent to the reduced volume. Cementation (calcite, silica, and iron oxide) typically reduces porosity in proportion to the cement volume [59]. Consequently, the remaining intergranular pores in sandstone today (V_3) have undergone compaction and cementation during the burial process in clastic reservoirs, and the calculated formula is as follows:

$$V_3 = \frac{P_1}{P_t} \times Q_m \tag{5}$$

$$V_{cc} = V_2 - V_3 \tag{6}$$

In the above formula, V_3 represents the porosity after compaction and cementation, expressed in %; V_{cc} represents the porosity reduction caused by cementation, expressed in %. The calculation results show an average decrease of 11.8% in the porosity of the Enping Formation, ranging from 0 to 11.1%. This study indicates that cementation significantly influences the reservoir in the Enping Formation, resulting in a primary pore loss rate ranging from 2.1 to 28.7% based on the observed relationship between the intergranular volume (IGV) and cement content in sandstone reservoirs (Figure 8).

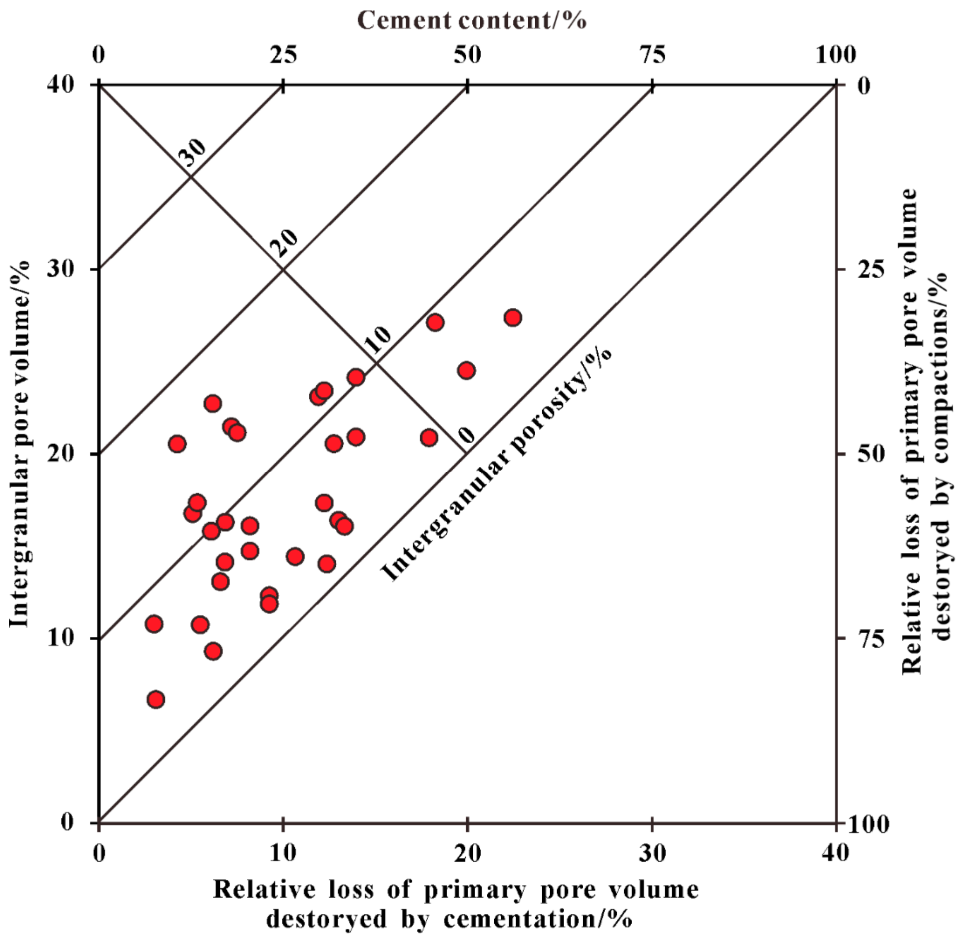

Figure 8. Relationship between intergranular volume and cement content in Enping Formation, Huizhou Depression.

5.3. Impact of Dissolution on Reservoir Quality

Acidic and alkaline corrosion is crucial in regulating reservoir space within deep sandstone reservoirs [60–63]. The dissolution of acidic fluids affects the deep, low-permeability reservoir of the Enping Formation in the study area. This leads to the dissolution of soluble components such as clastic particles, calcareous materials, and tuffaceous interstitials under the influence of organic acids [38,54]. As a result, many secondary pore spaces are formed, significantly improving the physical properties of the deep, low-permeability reservoir. This process causes an increase in secondary porosity, which is equivalent to the reservoir's remaining secondary porosity. We express the increased porosity (V_4) resulting from the dissolution of the Enping Formation as follows:

$$V_4 = \frac{P_2 + P_3}{P_t} \times Q_m \tag{7}$$

In the formula above, P_2 represents the face rate of dissolved pores within the grain calculated using thin sections observed under a microscope, expressed in %; P_3 represents the intergranular dissolved pore face rate, expressed in %; and V_4 represents the porosity increase caused by dissolution, expressed in %. The results show an average increase in porosity of 1.2–26.4%, with an average of 8.9%, due to dissolution in deep, low-permeability reservoirs in the Enping Formation. The calculation of the porosity of Enping Formation sandstone reveals that the loss in porosity due to calcareous, argillaceous, siliceous, and ferric cementation accounts for 12.3% of the reservoir volume. An analysis of dissolution illustrated an increase in porosity ranging from 1.4 to 25.6%, with an average value of 10.1%; compaction results in a reduction in reservoir porosity ranging from 11.8% to 27.2%, with an average value of 18.9%. We observe that mechanical compaction is the primary factor influencing the reservoir's physical properties, causing significantly more damage to the original porosity than cementation processes. According to existing research, there were two stages of oil and gas filling in the Enping Formation reservoir in the study area: 12.0–7.5 Ma and 6.5–0 Ma, with the second stage being the primary phase. The first stage, hydrocarbon charging, occurred during the A stage of the middle diagenetic phase. The reservoir was buried at a depth of over 3300 m, resulting in strong acid dissolution and increasing the porosity to 18.6%, and the layout of oil and gas accumulated. Around 6.5 Ma, the reservoir underwent a second oil and gas filling stage. Due to a combination of chemical compaction, calcareous cementation, and clay mineral cementation, the porosity of the reservoir decreased to about 6.3%, rendering deep reservoirs relatively dense. Industrial oil and gas reservoirs can form under large-scale oil and gas accumulation conditions. A comprehensive analysis of the matching relationship between oil and gas charging and the evolution of reservoir pores shows that the deep reservoir type in this area follows a "tight first, then accumulation" pattern.

6. Conclusions

(1) It was found that the reservoirs of the Enping Formation have a high quartz content and are mainly composed of feldspar quartz sandstone ($Q_{76}F_{16}L_8$) and lithic quartz sandstone ($Q_{67}F_{15}L_{18}$). The reservoir space primarily includes intergranular pores, dissolution pores, and microfractures, but the primary pores and dissolution pores are the main ones, and the two kinds of reservoir space account for more than 70%. The porosity of the core ranges from 1.1 to 19.8%, while its permeability ranges from 0.0017 to 612.02 $\times 10^{-3}$ μm^2. The reservoir is characterized by low porosity and permeability.

(2) The diagenetic evolution sequence of the Enping Formation reservoir can be summarized as follows: early diagenetic stage A (IA): mechanical compaction/chlorite film $\rightarrow$ early diagenetic stage B (IB): mechanical compaction/tuffaceous alteration/feldspar dissolution $\rightarrow$ middle diagenetic stage A (IIA): mechanical compaction/calcite cementation/feldspar dissolution/debris dissolution/kaolinite consolidation $\rightarrow$ middle diagenetic stage B (IIB): chemical compaction/dolomite cement/pore chlorite/quartz enlargement.

(3) The deep low-permeability Enping Formation reservoir space is significantly influenced by diagenesis, with compaction resulting in a porosity reduction ranging from 12.5 to 27.2% (an average of 18.9%). Cementation reduced the pore volume by 2.1–28.7% (average of 11.7%), while dissolution increased porosity by 1.4–25.6% (average of 10.1%).

Author Contributions: Conceptualization, Methodology, Software, and Writing—Original Draft, S.J. (Shan Jiang); Formal Analysis and Validation, R.G.; Data Curation, S.J. (Shuyu Jiang); Investigation and Writing—Review and Editing, J.C. All authors have read and agreed to the published version of the manuscript.

Funding: This research was financially supported by the National Natural Science Foundation of China (No. 42002150), the Open Foundation of the Cooperative Innovation Center of Unconventional Oil and Gas, Yangtze University (Ministry of Education & Hubei Province) (No. UOG2024–12), the Open Foundation Project of the Key Laboratory of Polar Geology and Marine Mineral Resources (China University of Geosciences, Beijing, China), the Ministry of Education (No. PGMR–2023–201), and the National Key Research Program of China (No. 2017ZX05032–002).

Institutional Review Board Statement: Not applicable.

Informed Consent Statement: Not applicable.

Data Availability Statement: All data and materials are available upon request from the corresponding author. The data are not publicly available due to ongoing research using a part of the data.

Conflicts of Interest: The authors declare no conflicts of interest.

References

1. Bhuyan, D.; Borgohain, P.; Bezbaruah, D. Diagenesis and Reservoir Quality of Oligocene Barail Group of Upper Assam Shelf, Assam and Assam Arakan Basin, India. *J. Asian Earth Sci.* **2022**, *7*, 100100. [CrossRef]
2. Risha, M.; Tsegab, H.; Rahmani, O.; Douraghi, J. The Impact of Clay Minerals on the Porosity Distribution of Clastic Reservoirs: A Case Study from the Labuan Island, Malaysia. *Appl. Sci.* **2023**, *13*, 3427. [CrossRef]
3. Samakinde, C.; Opuwari, M.; van Bever Donker, J.M. The Effects of Clay Diagenesis on Petrophysical Properties of the Lower Cretaceous Sandstone Reservoirs, Orange Basin, South Africa. *S. Afr. J. Geol.* **2016**, *119*, 187–202. [CrossRef]
4. He, Y.; Guo, H.; Lan, H.; Ling, C.; Fu, M. The Effect of Single Sandstone Stacking Pattern on the Sandstone Reservoir Physical Properties—A Case Study from the Shanxi Formation in the Daniudi Area, Northeastern Ordos Basin. *Energies* **2022**, *15*, 4740. [CrossRef]
5. Hu, W.; Bao, J.; Hu, B. Trend and Progress in Global Oil and Gas Exploration. *Pet. Explor. Dev.* **2013**, *40*, 439–443. [CrossRef]
6. Anjos, S.M.C.; Sombra, C.L.; Spadini, A.R. Petroleum Exploration and Production in Brazil: From Onshore to Ultra-Deepwaters. *Pet. Explor. Dev.* **2024**, *51*, 912–924. [CrossRef]
7. Neupane, B. Editorial: Advances in Exploration and Exploitation of Deep and Ultra-Deep Shale Oil and Gas. *Front. Earth Sci.* **2023**, *11*, 1205217. [CrossRef]
8. Prischepa, O.M.; Kireev, S.B.; Nefedov, Y.V.; Martynov, A.V.; Lutsky, D.S.; Krykova, T.N.; Sinitsa, N.; Xu, R. Theoretical and Methodological Approaches to Identifying Deep Accumulations of Oil and Gas in Oil and Gas Basins of the Russian Federation. *Front. Earth Sci.* **2023**, *11*, 1192051. [CrossRef]
9. Tarasenko, A.K.; Alekseeva, A.K.; Khohlova, Y.N.; Inshakova, N.Y. Tectonic Basis for Oil and Gas Potential in the North Kara Prospective Oil and Gas Region (Western Arctic, Russia). *Geotectonics* **2024**, *58*, 196–205. [CrossRef]
10. Li, Z.; Wu, S.; Xia, D.; Zhang, X.; Huang, M. Diagenetic Alterations and Reservoir Heterogeneity within the Depositional Facies: A Case Study from Distributary-Channel Belt Sandstone of Upper Triassic Yanchang Formation Reservoirs (Ordos Basin, China). *Mar. Pet. Geol.* **2017**, *86*, 950–971. [CrossRef]
11. Zhi, D.; Kang, X.; Qin, Z.; Tang, Y.; Cao, J.; Hu, R. Fluid-Rock Interactions and Porosity Genesis in Deep Clastic Reservoirs: A Perspective of Differential Oil Charge Intensity. *Mar. Pet. Geol.* **2022**, *137*, 105508. [CrossRef]
12. Saha, A.; Bhattacharya, B. Controls on Near-Surface and Burial Diagenesis of a Syn-Rift Siliciclastic Rock Succession: A Study from Permian Barren Measures Formation, Southern India. *Sediment. Geol.* **2022**, *436*, 106170. [CrossRef]
13. Cao, Y.; Yuan, G.; Wang, Y.; Zan, N.; Jin, Z.; Liu, K.; Xi, K.; Wei, Y.; Sun, P. Successive Formation of Secondary Pores via Feldspar Dissolution in Deeply Buried Feldspar-Rich Clastic Reservoirs in Typical Petroliferous Basins and Its Petroleum Geological Significance. *Sci. China Earth Sci.* **2022**, *65*, 1673–1703. [CrossRef]
14. Bello, A.M.; Jones, S.; Gluyas, J.; Acikalin, S.; Cartigny, M. Role Played by Clay Content in Controlling Reservoir Quality of Submarine Fan System, Forties Sandstone Member, Central Graben, North Sea. *Mar. Pet. Geol.* **2021**, *128*, 105058. [CrossRef]
15. Okunuwadje, S.E.; Bowden, S.A.; Macdonald, D.I.M. Diagenesis and Reservoir Quality in High-Resolution Sandstone Sequences: An Example from the Middle Jurassic Ravenscar Sandstones, Yorkshire CoastUK. *Mar. Pet. Geol.* **2020**, *118*, 104426. [CrossRef]
16. Shi, Y.; Liu, Z.; Wang, S.; Wu, J.; Liu, X.; Hu, Y.; Chen, S.; Feng, G.; Wang, B.; Wang, H. Genetic Mechanism and Main Controlling Factors of High-Quality Clastic Rock Reservoirs in Deep and Ultradeep Layers: A Case Study of Oligocene Linhe Formation in Linhe Depression, Hetao Basin, NW China. *Pet. Explor. Dev.* **2024**, *51*, 548–562. [CrossRef]
17. Aro, O.E.; Jones, S.J.; Meadows, N.S.; Gluyas, J.; Charlaftis, D. The Importance of Facies, Grain Size and Clay Content in Controlling Fluvial Reservoir Quality—An Example from the Triassic Skagerrak Formation, Central North Sea, UK. *Pet. Geosci.* **2023**, *29*, petgeo2022-043. [CrossRef]

18. Qiao, J.; Zeng, J.; Jiang, S.; Wang, Y. Impacts of Sedimentology and Diagenesis on Pore Structure and Reservoir Quality in Tight Oil Sandstone Reservoirs: Implications for Macroscopic and Microscopic Heterogeneities. *Mar. Pet. Geol.* **2020**, *111*, 279–300. [CrossRef]
19. Li, M.; Guo, Y.; Li, Z.; Wang, H. The Diagenetic Controls of the Reservoir Heterogeneity in the Tight Sand Gas Reservoirs of the Zizhou Area in China's East Ordos Basin: Implications for Reservoir Quality Predictions. *Mar. Pet. Geo.* **2020**, *112*, 104088. [CrossRef]
20. Yıldız, G.; Yılmaz, İ.Ö. Reservoir Heterogeneity of Ordovician Sandstone Reservoir (Bedinan Formation, SE Turkey): Diagenetic and Sedimentological Approaches. *Mar. Pet. Geol.* **2020**, *118*, 104444. [CrossRef]
21. Hakimi, M.H.; Shalaby, M.R.; Abdullah, W.H. Diagenetic Characteristics and Reservoir Quality of the Lower Cretaceous Biyadh Sandstones at Kharir Oilfield in the Western Central Masila Basin, Yemen. *J. Asian Earth Sci.* **2012**, *51*, 109–120. [CrossRef]
22. Hart, B.S.; Schieber, J.; Kalinec, J. Clay Diagenesis and Overpressure Development in Upper Cretaceous and Tertiary Shales of South Texas. *Mar. Pet. Geol.* **2023**, *147*, 105978. [CrossRef]
23. Niegel, S.; Franz, M. Depositional and Diagenetic Controls on Porosity Evolution in Sandstone Reservoirs of the Stuttgart Formation (North German Basin). *Mar. Pet. Geol.* **2023**, *151*, 106157. [CrossRef]
24. Azzam, F.; Blaise, T.; Patrier, P.; Abd Elmola, A.; Beaufort, D.; Portier, E.; Brigaud, B.; Barbarand, J.; Clerc, S. Diagenesis and Reservoir Quality Evolution of the Lower Cretaceous Turbidite Sandstones of the Agat Formation (Norwegian North Sea): Impact of Clay Grain Coating and Carbonate Cement. *Mar. Pet. Geol.* **2022**, *142*, 105768. [CrossRef]
25. Zhai, C.; Lv, C.; Gao, R.; Li, F.; Xie, J.; Yu, S.; Zhang, Z.; Mou, Y.; Wang, H. Lower Limit of Effective Reservoir Physical Properties and Controlling Factors of Medium-Deep Clastic Reservoirs: A Case Study of the Dawangzhuang Area in Raoyang Sag, Bohai Bay Basin. *J Pet. Explor. Prod. Technol.* **2023**, *13*, 1283–1298. [CrossRef]
26. Dutton, S.P.; Loucks, R.G. Diagenetic Controls on Evolution of Porosity and Permeability in Lower Tertiary Wilcox Sandstones from Shallow to Ultradeep (200–6700 m) Burial, Gulf of Mexico Basin, USA. *Mar. Pet. Geol.* **2010**, *27*, 69–81. [CrossRef]
27. Jin, F.; Zhang, K.; Wang, Q.; Niu, X.; Yu, Z.; Bai, G.; Zhao, X. Formation Mechanisms of Good-Quality Clastic Reservoirs in Deep Formations in Rifted Basins: A Case Study of Raoyang Sag in Bohai Bay Basin, East China. *Pet. Explor. Dev.* **2018**, *45*, 264–272. [CrossRef]
28. Peltz, M.; Jacob, A.; Grathoff, G.H.; Enzmann, F.; Kersten, M.; Warr, L.N. A FIB-SEM Study of Illite Morphology in Aeolian Rotliegend Sandstones: Implications for Understanding the Petrophysical Properties of Reservoir Rocks. *Clays Clay Min.* **2022**, *70*, 84–105. [CrossRef]
29. Virolle, M.; Brigaud, B.; Fenies, H.; Bourillot, R.; Portier, E.; Patrier, P.; Derriennic, H.; Beaufort, D. Preservation and Distribution of Detrital Clay Coats in a Modern Estuarine Heterolithic Point Bar in the Gironde Estuary (Bordeaux, France). *J. Sediment. Res.* **2021**, *91*, 812–832. [CrossRef]
30. Umar, M.; Friis, H.; Khan, A.S.; Kassi, A.M.; Kasi, A.K. The Effects of Diagenesis on the Reservoir Characters in Sandstones of the Late Cretaceous Pab Formation, Kirthar Fold Belt, Southern Pakistan. *J. Asian Earth Sci.* **2011**, *40*, 622–635. [CrossRef]
31. Yan, Z.; Yang, Y.; Li, W.; Wang, Y.; Xie, M.; Xiong, Q. Analysis of Sand Production Law and Key Factors of Offshore Weakly Cemented Unconsolidated Sandstone Reservoirs. *Fresenius Env. Bull.* **2021**, *30*, 6574–6580.
32. Ortiz-Orduz, A.; Rios-Reyes, C.A.; Vargas-Escudero, M.A.; Garcia-Gonzalez, M. Impact of Diagenesis on the Reservoir Rock Quality of the Cachiri Group Tight Sandstones in Cesar Sub Basin (Colombia): A Case of Study from ANH-CR-MONTECARLO 1X Well. *J. Nat. Gas Sci. Eng.* **2021**, *95*, 104138. [CrossRef]
33. Civitelli, M.; Ravidà, D.C.G.; Borrelli, M.; Criniti, S.; Falsetta, E. Diagenesis and Petrophysics of Miocene Sandstones within Southern Apennines Foreland, Italy. *Mar. Pet. Geol.* **2023**, *155*, 106411. [CrossRef]
34. Bjørlykke, K. Relationships between Depositional Environments, Burial History and Rock Properties. Some Principal Aspects of Diagenetic Process in Sedimentary Basins. *Sediment. Geol.* **2014**, *301*, 1–14. [CrossRef]
35. Amendola, U.; Perri, F.; Critelli, S.; Monaco, P.; Cirilli, S.; Trecci, T.; Rettori, R. Composition and Provenance of the Macigno Formation (Late Oligocene–Early Miocene) in the Trasimeno Lake Area (Northern Apennines). *Mar. Pet. Geol.* **2016**, *69*, 146–167. [CrossRef]
36. Civitelli, M.; Critelli, S.; Ingersoll, R.V. Interpreting Post-Depositional Alterations in Deep-Marine Sandstones: Butano Sandstone, Central California USA. *Mar. Pet. Geol.* **2024**, *163*, 106733. [CrossRef]
37. Xu, C.; Gao, Y.; Liu, J.; Peng, G.; Liu, P.; Xiong, W.; Song, P. Discovery and Inspiration of Large- and Medium-Sized Glutenite-Rich Oil and Gas Fields in the Eastern South China Sea: An Example from Paleogene Enping Formation in Huizhou 26 Subsag, Pearl River Mouth Basin. *Pet. Explor. Dev.* **2024**, *51*, 15–30. [CrossRef]
38. Long, G.S.; Shi, H.S.; Zheng, R.C.; Du, J.Y.; Liu, J.; Zhang, X.Y. Diagenesis and porosity evolution of deep reservoirs in Huizhou depression, Pearl River Mouth basin. *Yanshi Kuangwuxue Zazhi (Acta Petrol. Et Mineral.)* **2011**, *30*, 665–673.
39. Jiang, Z.; Zhu, J.; Deng, H.; Hou, D. Petroleum System and Hydrocarbon Accumulation Characteristics in the Wenchang and Enping Formations in the Huizhou Sag, Pearl River Mouth Basin, China. *Energy Explor. Exploit.* **2012**, *30*, 351–371. [CrossRef]
40. Zhao, Z.; Sun, Z.; Qiu, N.; Zhao, M.; Zhang, J.; Li, F.; Lin, J.; Young Lee, E. The Paleo-Lithospheric Structure and Rifting-Magmatic Processes of the Northern South China Sea Passive Margin. *Gondwana Res.* **2023**, *120*, 162–174. [CrossRef]
41. Gao, J.; Wu, S.; McIntosh, K.; Mi, L.; Yao, B.; Chen, Z.; Jia, L. The Continent–Ocean Transition at the Mid-Northern Margin of the South China Sea. *Tectonophysics* **2015**, *654*, 1–19. [CrossRef]

42. Shi, H.S.; He, M.; Zhang, L.; Yu, Q.; Pang, X.; Zhong, Z.; Liu, L. Hydrocarbon geology, accumulation pattern and the next exploration strategy in the eastern Pearl River Mouth Basin. *China Offshore Oil Gas* **2014**, *26*, 11–22.
43. Jiang, H.; Pang, X.; Shi, H.; Yu, Q.; Cao, Z.; Yu, R.; Chen, D.; Long, Z.; Jiang, F. Source Rock Characteristics and Hydrocarbon Expulsion Potential of the Middle Eocene Wenchang Formation in the Huizhou Depression, Pearl River Mouth Basin, South China Sea. *Mar. Pet. Geo.* **2015**, *67*, 635–652. [CrossRef]
44. Liu, E.; Chen, S.; Yan, D.; Deng, Y.; Wang, H.; Jing, Z.; Pan, S. Detrital Zircon Geochronology and Heavy Mineral Composition Constraints on Provenance Evolution in the Western Pearl River Mouth Basin, Northern South China Sea: A Source to Sink Approach. *Mar. Pet. Geol.* **2022**, *145*, 105884. [CrossRef]
45. Geological Evaluating Methods for Tight Sandstone Gas. Available online: https://transcustoms.cn/GB_standards/GB_standards_cn.asp?code=SY/T%206832-2011 (accessed on 11 December 2024).
46. Blanco, G.; Abre, P.; Ferrizo, H.; Gaye, M.; Gamazo, P.; Ramos, J.; Alvareda, E.; Saracho, A. Revealing Weathering, Diagenetic and Provenance Evolution Using Petrography and Geochemistry: A Case of Study from the Cretaceous to Cenozoic Sedimentary Record of the SE Chaco-Parana Basin in Uruguay. *J. South Am. Earth Sci.* **2021**, *105*, 102974. [CrossRef]
47. Baruah, M.; Pandey, N. Petrological and Geochemical Characterization of Miocene Tipam Sandstone in Parts of Cachar Fold Belt, Northeast India. *J. Geol. Soc. India* **2023**, *99*, 917–928. [CrossRef]
48. Ahmad, S.; Wadood, B.; Khan, S.; Ahmed, S.; Ali, F.; Saboor, A. Integrating the Palynostratigraphy, Petrography, X-Ray Diffraction and Scanning Electron Microscopy Data for Evaluating Hydrocarbon Reservoir Potential of Jurassic Rocks in the Kala Chitta Range, Northwest Pakistan. *J. Pet. Explor. Prod. Technol.* **2020**, *10*, 3111–3123. [CrossRef]
49. Putnis, A. Fluid–Mineral Interactions: Controlling Coupled Mechanisms of Reaction, Mass Transfer and Deformation. *J. Petrol.* **2021**, *62*, egab092. [CrossRef]
50. Kim, Y.; Lee, C.; Lee, E.Y. Numerical Analysis of Sedimentary Compaction: Implications for Porosity and Layer Thickness Variation. *J. Geol. Soc. Korea* **2018**, *54*, 631–664. [CrossRef]
51. Worden, R.H.; Utley, J.E.P. Automated Mineralogy (SEM-EDS) Approach to Sandstone Reservoir Quality and Diagenesis. *Front. Earth Sci.* **2022**, *10*, 794266. [CrossRef]
52. Xiong, Z.; Cao, Y.; Liang, C.; Liu, K.; Wang, G.; Zhu, R.; Lei, P.; Wang, Y. Origin and Significance of Authigenic Quartz and Albite in Lacustrine Calcareous Fine-Grained Sedimentary Rocks. *Mar. Pet. Geol.* **2022**, *143*, 105799. [CrossRef]
53. Chang, S.; Chen, D.; Wang, C.; Wang, Q.; Liu, Z.; Wang, F.-w. Preservation mechanism and model of primary pore diagenesis in deep reservoirs: Taking the Enping Formation and Wenchang Formation in the south of Huizhou Sag, Pearl River Mouth Bairn as examples. *J. Northeast Pet. Univ.* **2022**, *46*, 72.
54. Wang, Z.; Luo, X.; Lei, Y.; Zhang, L.; Shi, H.; Lu, J.; Cheng, M.; Liu, N.; Wang, X.; He, Y.; et al. Impact of Detrital Composition and Diagenesis on the Heterogeneity and Quality of Low-Permeability to Tight Sandstone Reservoirs: An Example of the Upper Triassic Yanchang Formation in Southeastern Ordos Basin. *J. Pet. Sci. Eng.* **2020**, *195*, 107596. [CrossRef]
55. Limarino, C.O.; Giordano, S.R.; Rodriguez Albertani, R.J.; Ciccioli, P.L.; Bodan, F. Patterns and Origins of the Porosity in the Productive Reservoirs of the Upper Part of the Chubut Group, Southern Flank of the Golfo de San Jorge Basin, Patagonia Argentina. *J. South Am. Earth Sci.* **2020**, *98*, 102480. [CrossRef]
56. Wang, Z.; Liu, Y.; Lu, S.; Lin, L.; Zhou, N.; Liu, Y. Differential Development Characteristics of Secondary Pores and Effects on Pore Structure and Movable Fluid Distribution in Tight Gas Sandstones in the Lower Permian, Northeastern Ordos Basin, China. *Geoenergy Sci. Eng.* **2023**, *224*, 211580. [CrossRef]
57. The division of Diagenetic Stages in Clastic Rocks. Available online: https://www.gbstandards.org/China_industry_standard_english.asp?code=SY/T%205477-2003 (accessed on 11 December 2024).
58. Beard, D.C.; Wey, P.K. Influence of texture on porosity and permeability of unconsolidated sand. *AAPG Bull.* **1973**, *57*, 349–369.
59. Lundegard, P.D. Sandstone porosity loss-a "big picture" view of the importance of compaction. *J. Sediment. Res.* **1992**, *62*, 250–260. [CrossRef]
60. Vincent, B.; Waters, J.; Witkowski, F.; Daniau, G.; Oxtoby, N.; Crowley, S.; Ellam, R. Diagenesis of Rotliegend Sandstone Reservoirs (Offshore Netherlands): The Origin and Impact of Dolomite Cements. *Sediment. Geol.* **2018**, *373*, 272–291. [CrossRef]
61. Okunuwadje, S.E.; MacDonald, D.; Bowden, S. Diagenetic and Reservoir Quality Variation of Miocene Sandstone Reservoir Analogues from Three Basins of Southern California, USA. *J. Earth Sci.* **2020**, *31*, 930–949. [CrossRef]
62. Wang, J.; Zhou, L.; Liu, J.; Zhang, X.; Zhang, F.; Zhang, B. Acid-Base Alternation Diagenesis and Its Influence on Shale Reservoirs in the Permian Lucaogou Formation, Jimusar Sag, Junggar Basin, NW China. *Pet. Explor. Dev.* **2020**, *47*, 962–976. [CrossRef]
63. Li, C.; Guo, P.; Xu, J.; Zhong, K.; Wen, H. Influences of Different Alkaline and Acidic Diagenetic Environments on Diagenetic Evolution and Reservoir Quality of Alkaline Lake Shales. *Pet. Explor. Dev.* **2024**, *51*, 97–113. [CrossRef]